and integrating outward using Numerov's method. For large ζ, the calculated function is fitted to the asymptotic form (A6) (with 0.5% accuracy) to determine A.

The allowed absorption coefficient is proportional to [see Eq. (3.18)]

$$\sum_{\nu} |U_{\nu}(0)|^2 \delta(E-E_{\nu})$$

$$= 2\sum_{t,E'} \lim_{\xi\to 0,\zeta\to 0} \frac{|\chi_1(\xi;t_n,E')\chi_2(\xi;t_n,E')|^2}{\xi\zeta}$$

$$\times \delta(E-E'), \quad (A9)$$

where the factor of 2 is included for spin. In order to convert the sum over E' to an integral, we determine the density of states $\rho(E)=dn/dE$ by requiring that the wave function χ_2 [Eq. (A6)] be zero at $\zeta=L_2$ [i.e., $\frac{2}{3}f^{1/2}(\frac{1}{2}L_2)^{3/2}\sim n\pi$],

$$\rho(E') = \frac{dn}{dE'} = \frac{1}{\pi}\frac{L_2^{1/2}}{2f}. \quad (A10)$$

The resulting allowed absorption coefficient is

$$K_A = \frac{4\pi^2 e^2}{m^2 c\eta'(\omega)\omega}\frac{2\sqrt{L_2}}{\pi(2f)^{1/2}}$$

$$\times\sum \lim_{\xi\to 0,\zeta\to 0} \frac{|\chi_1(\xi;t_n,E)\chi_2(\zeta;t_n,E)|^2}{\xi\zeta}. \quad (A11)$$

If we follow Ralph and we do not normalize χ_1 and χ_2 according to Eqs. (A2) and (A7) but instead define "unnormalized" χ_{1-UN} and χ_{2-UN} by Eqs. (A1) and (A8), then we get Ralph's formula

$$K_A = [4\pi^2 e^2/m^2 c\eta'(\omega)\omega]2|U(0)|^2 S(E), \quad (A12)$$

where

$$|U(0)|^2 S(E) = \frac{1}{Ra^3}\sum_{n=0}^{\infty}\left(\pi^2 f^{1/2}\int_0^{\infty}\frac{\chi_{1-UN}^2}{\xi}\right.$$

$$\left.\times(\xi;t_n,E)d\xi A^2(t_n,E)\right)^{-1}. \quad (A13)$$

In Eqs. (A12) and (A13), we have restored cgs units, with the understanding that all quantities to the right of the summation in Eq. (A13) are unitless. Equation (A12) differs from Ralph's result by a factor of 2, presumably due to spin.

X-Ray Scattering by Very Defective Lattices*

Sabri Ergun

Solid State Physics, Pittsburgh Coal Research Center, Bureau of Mines,
U. S. Department of the Interior, Pittsburgh, Pennsylvania 15213

(Received 17 April 1969; revised manuscript received 4 December 1969)

There is evidence to indicate that some diffusely scattering substances are essentially highly defective lattices rather than made up of small domains diffracting incoherently with respect to each other. Equations have been derived for the diffraction profiles from such lattices; they are of a Cauchy type. Highly defective lattices are characterizable by a mean defect-free distance rather than a domain size. Several criteria are presented for distinguishing defect-broadening from domain or particle-size broadening, and procedures are outlined for the separation of strain and defect broadenings.

I. INTRODUCTION

D EFECTS in structures produce displacements in the positions of atoms. The effects of such displacements on the scattering intensities have been considered by several workers.[1-3] In the case of crystals, these treatments have been confined mostly to cases in which the concentration of defects is small. On the other hand, diffusely scattering substances are not treated as lattices containing a high defect concentration. Rather, they are commonly regarded as composed of small particles or crystallites or possessing some sort of a domain structure within the material such that the different domains diffract essentially incoherently with respect to one another.[4,5]

At least in carbons, the presence of small particles or crystallites having sizes indicated by the linewidths of their diffraction peaks is often not indicated by electron microscope observations[6-9] or small-angle x-ray scat-

[1] H. Ekstein, Phys. Rev. 68, 120 (1945).
[2] K. Huang, Proc. Roy. Soc. (London) A190, 102 (1947).
[3] D. T. Keating, J. Phys. Chem. Solids 29, 771 (1968).
[4] B. E. Warren and B. L. Averbach, J. Appl. Phys. 21, 595 (1950).
[5] B. E. Warren, *Progress in Metal Physics* (Pergamon Publishing Corp., New York, 1959), Vol. 8, pp. 147–202.
[6] H. Brusset, Compt. Rend. 225, 102 (1947); 227, 843 (1948).
[7] H. Kuroda, J. Colloid Sci. 12, 496 (1957).
[8] L. L. Ban, W. M. Hess, and F. J. Eckert, Carbon 6, 232 (1968).
[9] R. D. Heidenreich, W. M. Hess, and L. L. Ban, J. Appl. Cryst. 1, 1 (1968).
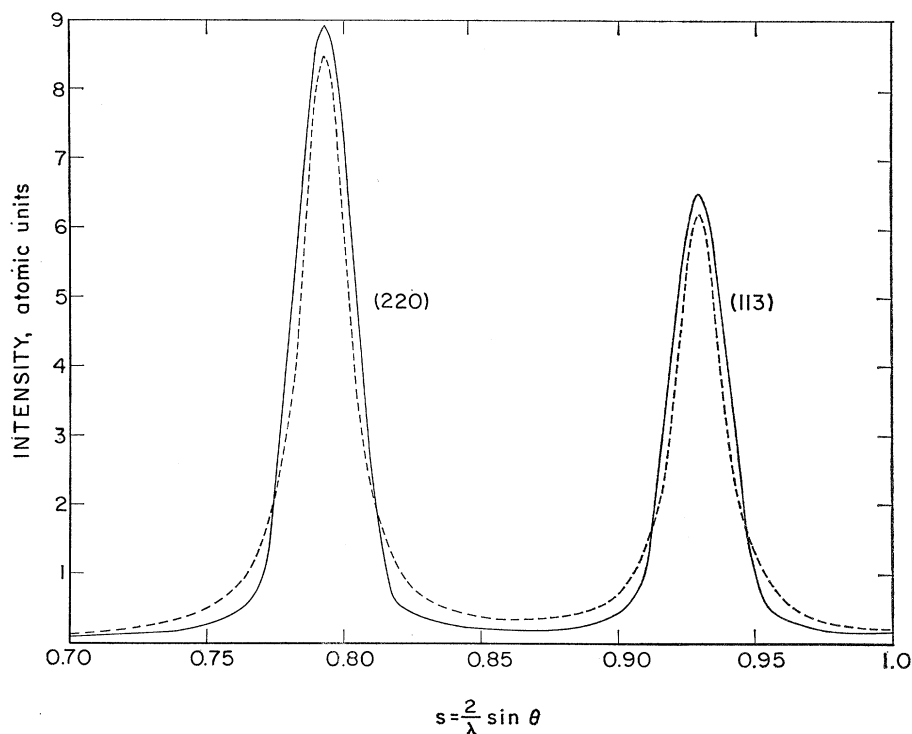
FIG. 1. Comparison of the calculated profiles of the (220) and (113) reflections of diamond assuming defect broadening (– – –) and particle-size broadening (—).

tering.[6,7,10,11] Improved atomic radial distribution curves of carbon blacks revealed the presence of interatomic distances much larger than those indicated by the linewidths of the $(hk0)$ reflections,[12,13] and careful analysis of the $(00l)$ reflections indicated the presence of extensive but faulty stacking rather than short stacks of small crystallites.[14,15] It was, therefore, proposed[13] that such substances are made up of large but defective domains rather than small domains diffracting incoherently with respect to one another. It appears that the case of very defective structures needs special attention.

II. THEORY

For simplicity, we consider a structure containing one kind of atom. The scattering intensity of a rigid lattice may generally be expressed as

$$j(s) = \frac{I(s)}{Nf^2} = 1 + \sum_q n(l_q)\langle\exp(i2\pi\mathbf{s}\cdot\mathbf{l}_q)\rangle, \quad |\mathbf{l}_q| \neq 0 \quad (1)$$

where $j(s)$ and $I(s)$ are the intensity in atomic and Thomson units, respectively; $s = (2\sin\theta)/\lambda$ is the magnitude of the diffraction vector $\mathbf{s}$; N is the total number

[10] J. Biscoe and B. E. Warren, Phys. Rev. **59**, 693 (1941).
[11] H. Brusset, J. Deveraux, and A. Guinier, Comp. Rend. **216**, 152 (1943).
[12] J. R. Townsend and S. Ergun, Carbon **6**, 19 (1968).
[13] S. Ergun, Carbon **6**, 141 (1968).
[14] S. Ergun and T. J. Gifford, J. Appl. Cryst. **1**, 13 (1968).
[15] S. Ergun and T. J. Gifford, J. Chim. Phys. Special Issue, 99 (1969).

of atoms in the structure; $n(l_q)$ is the total number of interatomic vectors of magnitude $l_q = |\mathbf{l}_q|$ divided by N, each vector being counted twice. In a lattice of infinite extent $n(l)$ is simply the number of neighboring atoms at a distance l to any atom. The variables l and $n(l)$ characterize the structure. Equations, in set notation, for l and $n(l)$ can be formulated for any given lattice, and examples are given in the Appendix for a graphite-like layer and for a diamond-type lattice, both of infinite and finite extent.

In a highly defective structure, it is necessary to distinguish between two types of interatomic distance vectors: (1) those that undergo large changes by random amounts and (2) those that experience small changes because of stress. For purposes of distinction, it is convenient to conceive a defect radius, i.e., a radius of a sphere of influence, and associate the first type with vectors which encounter defects and the second type with those that encounter no defects. We shall first consider the effect on the scattering intensity of large random displacements.

Random indeterminacies in interatomic distances, if sufficiently large, result in the elimination of their contribution to summation in Eq. (1). Essentially, what we are interested in is the modification of $n(l)$ in the equation. Consider a lattice of large extent in which defects are distributed randomly. If $g(l)$ is the probability that a distance l can be traversed without encountering a defect, the probability of traversing the distance $l + dl$ is $g(l + dl)$ and is given by the product of separate probabilities that distances l and dl will be
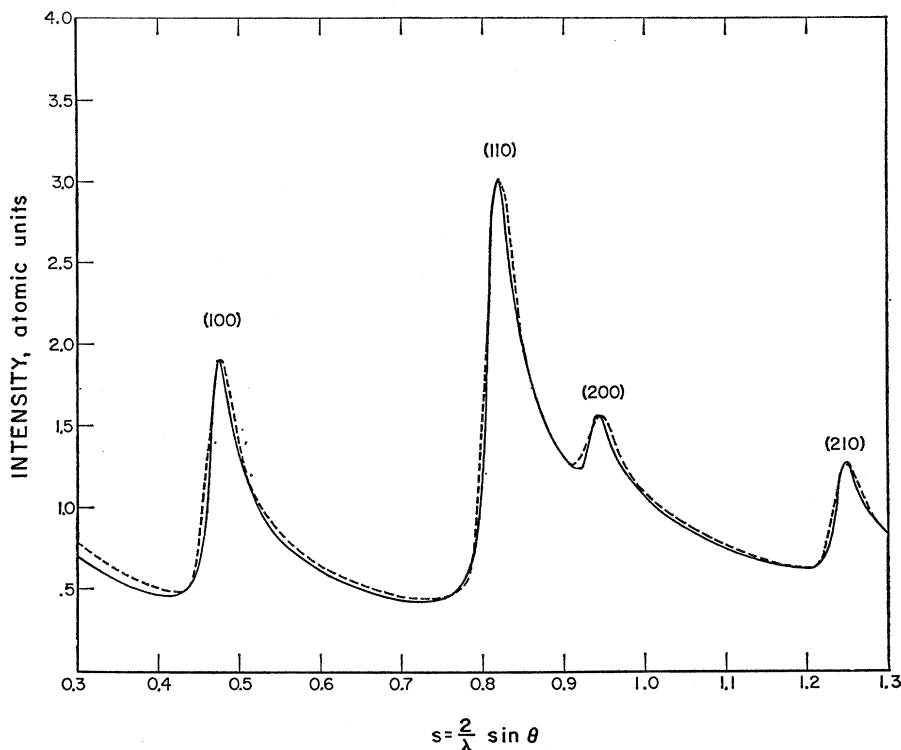
FIG. 2. Comparison of the calculated profiles of the (hk0) reflections of graphite assuming defect broadening (– – –) and particle-size broadening (—).

traversed without an encounter since the two probabilities are independent:

$$g(l+dl) = g(l) + [dg(l)/dl]dl = g(l)g(dl).$$

Consider a cylinder of unit cross-section area having a length dl. The probability $g(dl)$ of encountering a defect when the distance dl is traveled is given by the sum of the projections on the front surface of all defects lying within the cylinder divided by the front surface of unit area, i.e., $m\pi r^2$, m being the number of defects per unit volume, and r the defect radius. Hence, $g(dl) = 1 - m\pi r^2 dl$. Substitution in the preceding equation and integration yield

$$g(l) = e^{-m\pi r^2 l} = e^{-l/L}.$$ (2)

L, the reciprocal of $m\pi r^2$, has a significance analogous to mean free path; it can be termed the mean defect-free distance. If we are dealing with point defects having uniform radii r, an estimate of defect concentration can be made from the relation of L to the fraction of volume occupied by the defects. Designating the latter by P, we have

$$P = \tfrac{1}{3} m 4\pi r^3 = 4r/3L.$$

If $r \simeq 1$ Å and $L \simeq 50$ Å, then $P \simeq 0.03$, that is, the defect concentration is about 3%.

As postulated, $g(l)$ modifies $n(l)$ in Eq. (1); that is, the effective number of neighboring atoms at a distance l that contribute to the interference function of a defective lattice is $g(l)n(l)$. Obviously the use of Eq. (1)

to compute the scattering intensity of a large domain is prohibitive in that the number of terms in the summation is very large. However, when $n(l)$ in Eq. (1) is modified by $g(l)$, if L is sufficiently small, say < 40 Å, the number of terms that significantly contribute to the summation is greatly reduced, and the computation becomes feasible. For the powder patterns, the interference function is given by the well-known Debye equation

$$\langle e^{i2\pi s \cdot 1} \rangle = \tfrac{1}{2} \int_0^\pi e^{i2\pi s l \cos\alpha} \sin\alpha \, d\alpha = \frac{\sin 2\pi s l}{2\pi s l}.$$

Substituting the above equation into (1) and modifying it with $g(l)$, we obtain

$$j(s) = 1 + \sum_q g(l_q)n(l_q)\frac{\sin 2\pi s l_q}{2\pi s l_q}.$$ (3)

In Figs. 1 and 2 are shown, as dotted lines, the computed intensities of a diamond lattice ($L = 16$ Å) and a graphite layer ($L = 15$ Å), respectively, using Eq. (3). The formula for calculating the solid line is described below.

Equation (1) can also be used to compute the scattering intensities of lattices of finite extent provided expressions are derived that modify $n(l)$. It is readily recognized that the modifying expression depends upon the shape as well as the size of the particle or crystallite. For spherically shaped crystallites of radius R, the
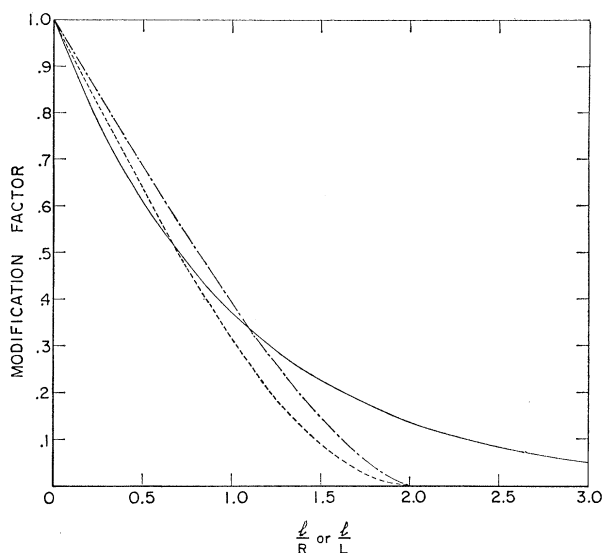
FIG. 3. Comparison of defect factor $e^{-l/L}$ (- - -) with particle-size factors

$$\epsilon_d = 2/\pi \left[\cos^{-1}\frac{l}{2R} - \frac{l}{2R}\left(1 - \frac{l^2}{4R^2}\right)^{1/2} \right] \quad (\text{— · —})$$

and

$$\epsilon_s = 1 - \tfrac{3}{2}(l/2R) + \tfrac{1}{2}(l/2R)^3 \quad (\text{— —}).$$

modifying factor is given by[16]

$$\epsilon_s(x) = 1 - \tfrac{3}{2}x + \tfrac{1}{2}x^3, \quad (\text{sphere}) \qquad (4)$$

for disk shaped layers the corresponding factor is given by[17]

$$\epsilon_d(x) = (2/\pi)[\cos^{-1}x - x(1-x^2)^{1/2}] \quad (\text{disk}). \qquad (5)$$

In the above equations, x is defined as $x = l/2R$. It is understood that we may refer to $\epsilon(x)$ as ϵ, $\epsilon(l)$, or $\epsilon(l/2R)$ as the clarity dictates.

In Fig. 3 are shown g, ϵ_s, and ϵ_d as a function of l/L or r/R. It is seen that there are differences in the mode of decrease of the average number of interatomic distances with increase in the distance. To observe the effects of the differences on the profiles of powder patterns, intensities have been computed, using Eq. (3) with $g(l)$ being replaced by $\epsilon(l)$, for a spherically shaped diamond crystallite ($R = 22$ Å) and a disk-shaped graphite layer ($R = 15$ Å). The results are shown in Figs. 1 and 2 as solid lines. The radius $R = 22$ Å for the diamond sphere was chosen to obtain a peak height comparable to that produced by the exponential factor. It is seen that there is a great similarity in the profiles produced by particle-size broadening and by defect broadening, especially for the graphite layer.

In Fig. 4 are shown the (002), (100), and (004) reflections of a carbon black before and after correction for instrumental broadening. The data were taken with Ag radiation using balanced Rh and Mo filters in trans-

mission geometry, 0.4° beam slit, 0.2° detector slit, and medium-resolution Soller slits. From the figure, it is seen that the differences observed in the plots of Figs. 1 and 2 are readily obscured by instrumental broadening. It is quite evident that a correction for instrumental broadening is a prerequisite for meaningful profile analyses.

The powder pattern profiles of the (hk0) reflections seen in Fig. 2 are typical of many carbons such as cokes, chars, blacks, etc. They are characterized by asymmetric peaks having large linewidths ($\sim$twice as much as those of crystalline reflections for the same dimension). Assume the intensities of a powder pattern of carbon are properly corrected for instrumental broadening and other experimental factors. Even then, the statistical errors, because of low scattering intensities of carbons, influence of the (00l) reflections, and the added diffuseness because of large linewidths, render it difficult to make a distinction between defect broadening and layer-size broadening based on curve-fitting experimental data over any single peak. Inasmuch as electron microscope observations and small-angle scattering do not support the presence of layers having sizes indicated by linewidths, we may conclude that the observed profiles are well explained by defect broadening.

III. PROFILES PRODUCED BY PARTICLE-SIZE AND DEFECT BROADENING

A direct confirmation of defect broadening is possible by a careful analysis of peak profiles. In the following treatment, it is assumed that the observed intensities are corrected for absorption, polarization, instrumental broadening, and Compton modified scattering, and are then normalized into atomic units.[18,19] Ideally suited for this purpose are samples that give rise to crystalline reflections. In this situation, the use of Eq. (1) with $n(l)$ modified with $g(l)$ or $\epsilon(l)$ becomes impractical when L or R is large, say >40 Å. It is then desirable to use the lattice-sum technique. In this regard, any given reflections from a crystallite may be considered as the (00l) reflections in terms of suitably chosen orthorhombic axes and the scattered intensity may be expressed in the form of a cosine series[5]:

$$j(s) = j_0(s)\left(1 + 2\sum_{q=1}^{N} A_q \cos 2\pi q \bar{z} s\right), \qquad (6)$$

where $\bar{z}$ is the mean height of the cell, $N\bar{z}$ is the maximum column height, NA_q is the number of cell pairs that are $q\bar{z}$ apart, and $j_0(s)$ represents the intensity of the (000) reflections (analogous to K of Warren and Averbach[4] or Ψ^2 of Houska and Warren[20]). If the

[16] L. H. Germer and A. H. White, Phys. Rev. 60, 447 (1941).
[17] S. Ergun, J. Appl. Cryst. (to be published).
[18] S. Ergun, J. Bayer, and W. Van Buren, J. Appl. Phys. 38, 340 (1967).
[19] S. Ergun, J. Appl. Phys. 40, 293 (1969).
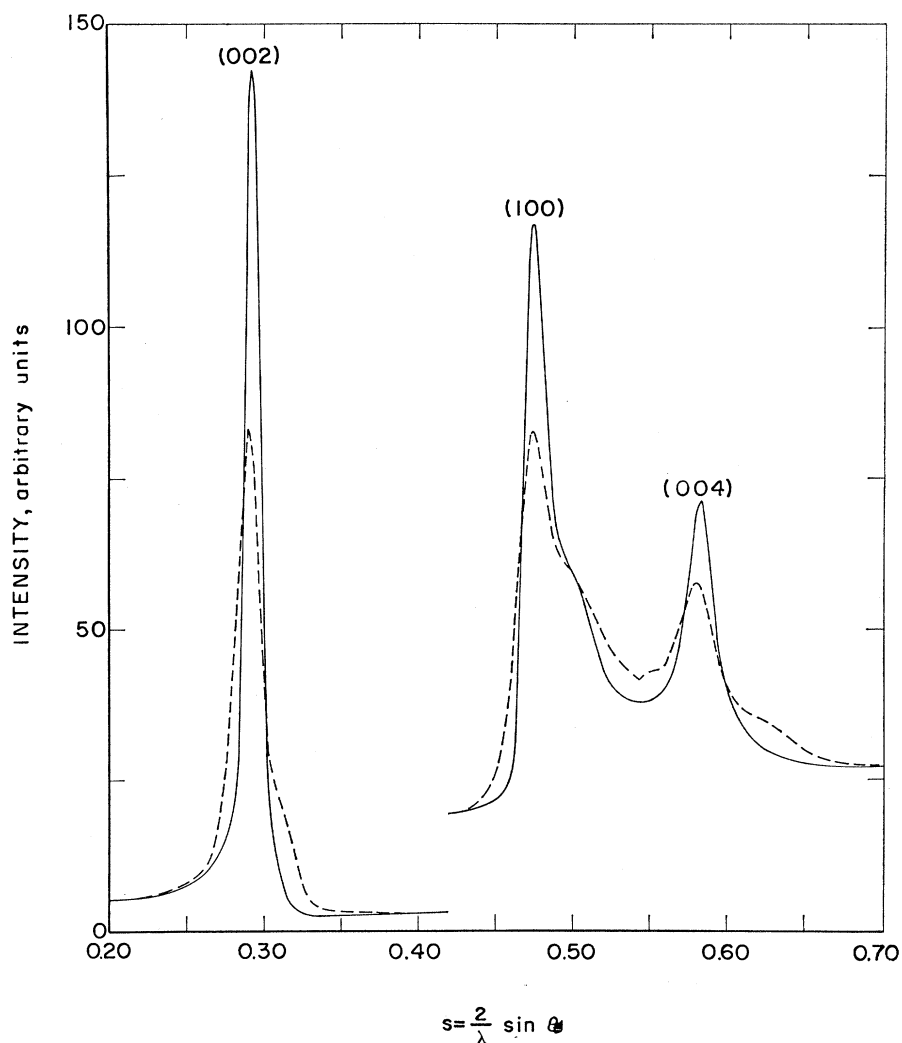[20] C. R. Houska and B. E. Warren, J. Appl. Phys. 25, 1053 (1954).

FIG. 4. Powder patterns of a heat-treated carbon black. Original intensity (– – –). Intensity corrected for instrumental broadening (—).

columns have uniform heights, A_q is given by[20]

$$A_q = \epsilon_d = 1 - q/N, \quad \text{(stacks)} \tag{7a}$$

and the stack height H by $H = N\bar{z}$. If the crystallites are spherically shaped, A_q is identical with ϵ_s defined in Eq. (4), i.e.,

$$A_q = \epsilon_s = 1 - 3q/2N + \tfrac{1}{2}(q/N)^3 \quad \text{(spheres)}. \tag{7b}$$

For disk-shaped layers the corresponding equation is

$$A_q = \epsilon_d = \frac{2}{\pi}\left[\cos^{-1}\frac{q}{N} - \frac{q}{N}\left(1 - \frac{q^2}{N^2}\right)^{1/2}\right] \quad \text{(disks)}. \tag{7c}$$

For the last two cases, the diameter $2R$ is related to N by $2R = N\bar{z}$. For the defective case considered in this study, A_q decreases exponentially with q, i.e.,

$$A_q = e^{-q/Q}, \quad \text{(defective lattice)} \tag{7d}$$

where Q is the mean number of defect-free cell sequences.

In the last case, the summation in Eq. (6) is extended to a very large number N.

From an inspection of Eq. (6), we observe that the peak occurs at $s = s_0 = 1/\bar{z}$; therefore, we may change the agruments of the cosine terms from $2\pi q\bar{z}s$ to $2\pi q\bar{z}(s - s_0)$. We further observe that the peak width $2|s - s_0|$ at half peak intensity is of the order of $1/N\bar{z}$ (cf. Scherrer equation[21]), and the peak is more or less confined to $s - s_0$ values such that $N\bar{z}|s - s_0| < 1$. If $N > 10$, we may replace the sum in Eq. (6) by an integral

$$i(s) = j(s)/j_0(s) = 2N\int_0^1 \epsilon(x)\cos[x\Phi(s)]\,dx \tag{8}$$

with

$$x = q/N, \quad \Phi(s) = 2\pi N\bar{z}(s - s_0). \tag{8'}$$

Simply denoting $\Phi(s)$ by Φ, the integrated equations for the three cases represented by Eqs. (7a)–(7c) take

[21] L. Bragg, *The Crystalline State, A General Survey* (G. Bell and Sons, London, 1919), Vol. 1, p. 189.

the forms, respectively,

$$i(s) = N[\sin(\Phi/2)/(\Phi/2)]^2, \quad \text{(stacks)} \quad (9a)$$

$$i(s) = (3N/4)\{8[1+(\Phi^2/2)-\cos\Phi-\Phi\sin\Phi]/\Phi^4\},$$
$$\text{(spheres)} \quad (9b)$$

$$i(s) = (8N/3\pi)[3\pi H_1(\Phi)/2\Phi^2] \quad \text{(disks)}. \quad (9c)$$

For the defective lattice carrying out the summation for $q=1$ to ∞, we obtain

$$i(s) = \frac{1+u}{1-u}\frac{(1-u)^2}{1+u^2-2u\cos2\pi\bar{z}s} \quad \text{(defective lattice)} \quad (9d)$$

with $u = e^{-1/Q}$. In Eq. (9c), H_1 is the Struve function of first order and is tabulated by Watson.[22] Since the argument of H_1 is less than 2π, the power series representation of $H_1(\Phi)/\Phi^2$ converges very rapidly, and numerical evaluation presents no problem.

If $Q>5$, the following simplifications may be made in Eq. (9d): $u\simeq1-1/Q$ and $\cos2\pi\bar{z}(s-s_0)\simeq1-2\pi^2\bar{z}^2(s-s_0)^2$. With these simplifications, Eq. (9d) assumes a Cauchy form:

$$i(s) = 2Q/\{1+[2\pi L(s-s_0)]^2\}, \quad (10)$$

where $L=Q\bar{z}$ is the mean defect-free distance. It is quite evident that if the intensity profiles are of a Cauchy type cf. Warren,[5] it is in accordance with the defect broadening proposed in this work. Equations (9a)–(9c) do not produce Cauchy-type profiles.

The preceding treatment has been confined to defective lattices of very large extent and to particles or domains having a uniform size. Equations for diffraction from small defective domains are readily obtained by modifying $n(l)$ in Eq. (1) with $g(l)\epsilon(l)$. When using Eq. (6), the summation is carried out to a finite value of N corresponding to the size of the domain. If Eq. (8) is modified by the exponential coefficient, it still remains integrable for the shapes considered in this study. To develop equations for a structure made up of small domains having a size distribution, an *a priori* knowledge of size distribution is essential. However, if the intensity profile has a Cauchy form, it is physically unrealistic to explain it in terms of a particle-size distribution, for it implies that the largest number of domains are those containing single cells. This can be shown as follows. Let there be a large number M of columns, and let the probability that a given column will contain m cells be e^{-cm}, c being a constant. There will be Me^{-cm} columns each containing m cells. The total number of cells N in the assembly is

$$N = M\sum_1^\infty me^{-cm} = \frac{Me^{-c}}{(1-e^{-c})^2}.$$

In the assembly, the total number of cell pairs that are

[22] G. N. Watson, *Theory of Bessel Functions* (Cambridge University Press, New York, 1952), pp. 328, 666–697.

q cells apart is given by

$$\sum_{m=q+1}^\infty M(m-q)e^{-cm} = \frac{Me^{-c}}{(1-e^{-c})^2}e^{-cq}.$$

This number divided by N is simply e^{-cq} and is the coefficient of the cosine term. If c is replaced by $1/Q$, the resulting equation will be identical with the defective case.

IV. RELATION OF PEAK HEIGHT TO PEAK WIDTH

A distinction between defect and more or less uniform particle-size broadening can be made in a rather simple manner if the intensities are corrected for strain broadening and Debye temperature effects. As shown below, the product of peak width and peak height is much lower for defect broadening. In Eqs. (9a)–(9d), the maximum values of $i(s)$ are factored, viz., N, $\frac{3}{4}N$, $8N/3\pi$, and $(1+u)/(1-u)\simeq2Q$, respectively. Thus the values of Φ at which the intensity is one-half the maximum are readily determined, viz., $\Phi=2.78, 3.475, \pi, 1$, respectively (for the defective case N is replaced by Q in defining Φ). It follows that in terms of Δs, the peak width at half-peak intensity, the peak heights are given by

$$i(s_0) = 2.78/\pi\bar{z}\Delta s, \quad \text{(stacks)} \quad (11a)$$

$$i(s_0) = 2.60/\pi\bar{z}\Delta s, \quad \text{(spheres)} \quad (11b)$$

$$i(s_0) = 2.67/\pi\bar{z}\Delta s, \quad \text{(disks)} \quad (11c)$$

$$i(s_0) = 2/\pi\bar{z}\Delta s \quad \text{(defective lattices)}. \quad (11d)$$

From a comparison of Eqs. (11a)–(11d), we observe that for the same linewidths, the defect broadening would give rise to a peak height much less than that produced by particle-size broadening; the ratios range from 0.72 to 0.77. This ratio permits distinction between defect and particle-size broadening. Further, numerical calculations show that Eqs. (9a)–(9c) yield very nearly the same profiles provided N's are chosen for each case such that they yield the same height or peak width.

V. BROADENING OF PROFILES BY STRAIN

Small displacements in the positions of atoms or cells are commonly referred to as strain or distortion. If the mean square displacements $\langle\xi^2\rangle$ are independent of the magnitude of the distance, their influence may be accounted by modifying Eqs. (1) and (6) with the Debye temperature factor $\exp(-\langle\xi^2\rangle s^2)$. The widths at half-peak intensity of the different reflections would not be altered significantly. Of particular interest is the case considered by Warren and co-workers[4,5,20] for small random displacements. If negative and positive strains occur with nearly equal probability, the strain effects are taken into account by multiplying the coefficients A_q in Eq. (6) with $\langle\cos2\pi s\bar{z}Z_q\rangle$, in which $\bar{z}Z_q$ is

the change in length of a column of length $q\bar{z}$. Further, if the strain distribution is Gaussian the expectation value of the cosine may be approximated by $\exp(-2\pi^2 s^2\bar{z}^2\langle Z_q^2\rangle)$. For the case in which the mean square displacement $\langle Z_q^2\rangle$ is made up of nearest-neighbor displacements $\langle Z_1^2\rangle$, then $\langle Z_q^2\rangle = q\langle Z_1^2\rangle$. Designating

$$\delta^2 = 2\pi^2\bar{z}^2\langle Z_1^2\rangle,$$

the coefficient A_q takes the form

$$A_q = e^{-\delta^2 s^2 q}\epsilon(q). \tag{12}$$

The Gaussian strain function has been discussed in detail by Warren. The results obtained in this study are in accordance with Warren's conclusions.

VI. SEPARATION OF STRAIN BROADENING

Inasmuch as the Gaussian strain coefficient is a function of q and s^2, the separation of strain broadening from defect or particle-size broadening is obviously facilitated if intensities are obtained for several orders of a given reflection. In the case of isotropic strain, all of the reflections can be used. A general prodecure of profile analysis is outlined by Warren.[5] It involves determination of the coefficients of the cosine terms A_q of intensities of a series of reflections. For a fixed value of q, a plot of $\ln A_q$ versus s_0^2 should be linear [cf. Eq. (12)]. The intercept of the line yields $\ln\epsilon(q)$ and the slope $-\delta^2 q$. It is clear that the slopes divided by q should be constant if $q\langle Z_1^2\rangle = \langle Z_q^2\rangle$ and if the strain distribution is Gaussian. Plots of $\epsilon(q)$ versus q should yield information about the nature of ϵ. This procedure is very general in that it involves no *a priori* assumptions as to the nature of A_q nor of $\langle Z_q^2\rangle$. However, the method is very sensitive to slight errors in the corrections and handling of data. Slight errors can result in large fluctuations in the coefficients obtained.

In the case of defect broadening, the resulting analytical expression for the interference function permits a direct and rather simple analysis of the profile. Modifying A_q [defined in Eq. (7d)] for the Gaussian distortion effects, we obtain

$$A_q = e^{-(1/Q+\delta^2 s^2)q}. \tag{13}$$

Substituting Eq. (13) into (6) and carrying out the summation to $q=\infty$, we obtain [cf. (9d)],

$$i(s) = \frac{1+u}{1-u}\frac{(1-u)^2}{1+u^2-2u\cos 2\pi\bar{z}s}, \tag{14}$$

in which

$$u = e^{-(1/Q+\delta^2 s^2)} \tag{15}$$

If $\delta^2 s^2 < 0.1$ and $Q > 10$, Eq. (14) takes a Cauchy form:

$$i(s) = \frac{2Q}{1+Q\delta^2 s^2}\left\{1\left/\left[1+\left(\frac{2\pi Q\bar{z}(s-s_0)}{1+Q\delta^2 s^2}\right)^2\right]\right.\right\}. \tag{16}$$

From Eq. (16), we note that the intensity is one-half

the maximum when

$$\Delta s = 2(s-s_{00l}) \simeq 1/\pi Q\bar{z} + (\delta^2/\pi\bar{z})s_{00l}^2, \tag{17}$$

in which s_{00l} corresponds to the peak position of the $(00l)$ reflections, Δs is the total width at half-peak intensity of the peak $(00l)$, $\bar{z} = 1/s_{00l}$, and $Q\bar{z} = L$, the mean defect-free distance. According to Eq. (15), if Δs for the different orders of reflection is plotted against s_{00l}^2, a straight line should be obtained with the slope and intercept yielding the values of δ^2 and Q. Once this is done, the observed profiles can be compared with those calculated using (14) or (16).

The direct prodecure outlined above is not necessarily confined to the case of defect broadening. When modified with $e^{-\delta^2 s^2 q}$, Eq. (8) takes the form

$$i(s) = 2N\int_0^1 \epsilon(x)e^{-vx}\cos\Phi x\, dx, \tag{18}$$

in which $v = N\delta^2 s^2$. The above equation is integrable for the three ϵ's discussed in this study. The resulting expressions are somewhat cumbersome. However, their examination revealed that a plot of Δs versus s_0^2 would yield a straight line following an initial curvature, the slope of the line being equal to $\sim 0.93\, \delta^2/\pi\bar{z}$. Furthermore, the initial slope of the curved section is equal to $0.5\, \delta^2/\pi\bar{z}$, i.e., about one-half of that of the straight section. Thus, extrapolation of the plot to zero abscissa can be made without introducing serious error. The intercept corresponds to $2.78/\pi N\bar{z}$ and to $3.475/\pi N\bar{z}$ for stacks and spheres, respectively.

Having determined the strain and defect or domain-size-coefficients, the peak heights should be examined for the effects of the Debye temperature factor if the peak heights should be used as a criterion for deciding whether defect or particle-size effects prevail. If the ratios of the observed heights to those calculated is independent of the order of reflection, it indicates negligible Debye temperature effects; otherwise, an exponential decrease with s_0^2 is expected. The degree of agreement between the observed and calculated results should permit an authentic distinction.

VII. DEFECTS IN CARBONS AND METALS

It was recently shown that the coefficients A_q of the $(00l)$ reflections of a raw and heat-treated carbon black showed exponential distributions.[14,15] In Fig. 5 are shown the observed and calculated powder-pattern intensities (in atomic units) of the (002) reflections of the heat-treated carbon black (cf. Fig. 4). From Fig. 5, it is seen that the profile is of Cauchy type, and Eq. (16) reproduces the observed profiles faithfully. The equation based on uniform stack height yields a high peak height when it matches the peak width or a broad peak when it matches the peak height (cf. Ref. 15). It may be argued that the observed profiles could be explained equally well by particle-size broadening if it is assumed
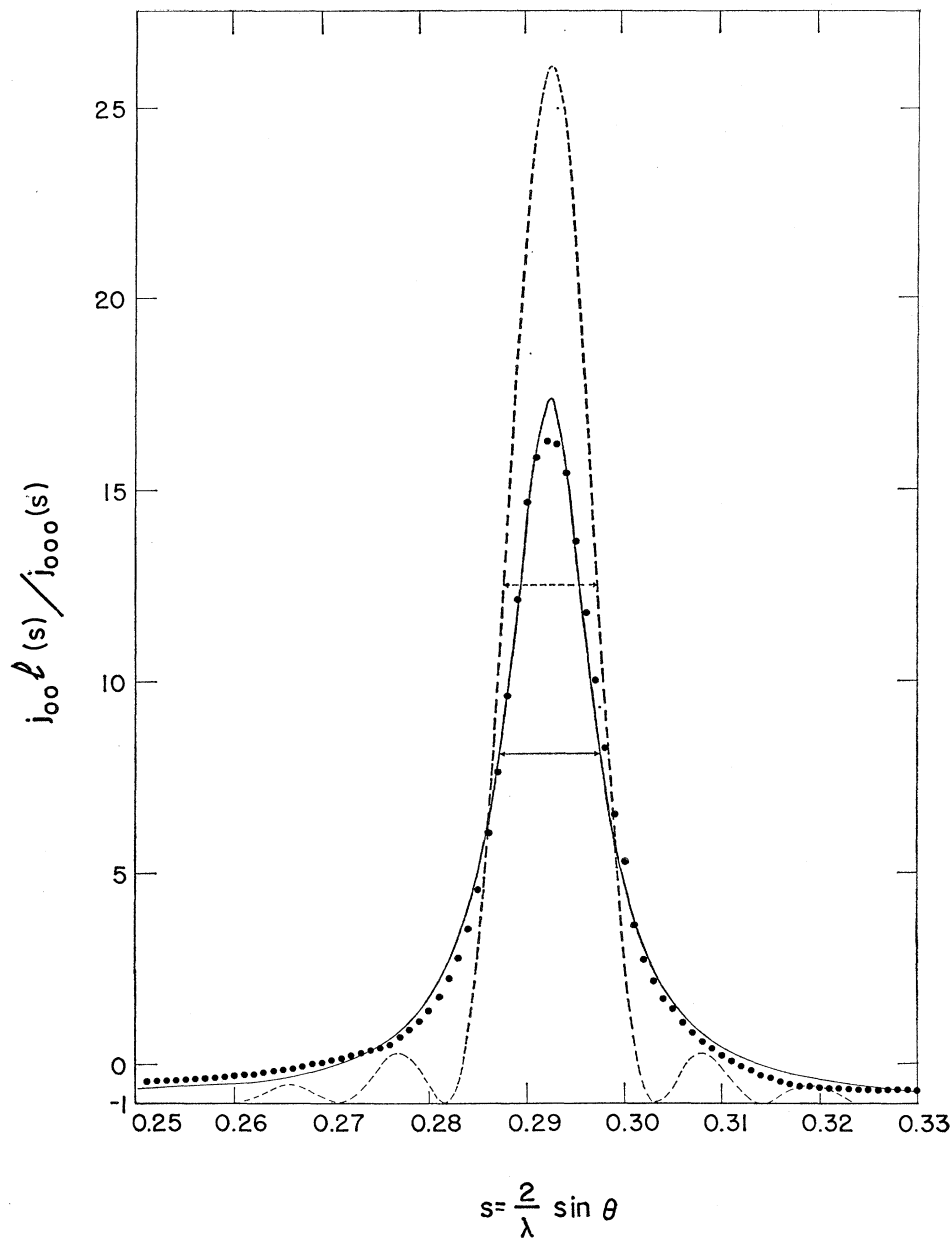
FIG. 5. Profile of the (002) reflection of a heat-treated carbon black. Experimental data (●), calculated assuming defect broadening (—), and calculated assuming particle-size broadening (– – –).

that stacking has an exponential distribution. However, we find direct support for extensive but faulty stacking from electron-microscope observations of carbons and additional support from heat-treatment studies. Progressive sharpening of the $(00l)$ reflections as a result of heat treatment is more plausibly explained by annealing stacking faults than by stacking of crystallites.

Analysis of the $(hk0)$ reflections from layered structures presents special problems; such structures tend to show preferred orientation. The powder patterns yield $(hk0)$ reflections that have long tails at the high-angle side. These tails usually have the profiles of other reflections superimposed on them. For this reason, it was found to be desirable to employ a sample that gave rise to crystalline $(hk0)$ reflections. Ideally suited for this purpose are pyrolytic carbons and carbon fibers that show a very high degree of preferred orientation. A parallel bundle of the latter, when placed in transmission geometry with fiber axis parallel to the diffraction vector, yields very symmetric $(hk0)$ reflections. If the layers are parallel to the fiber axis and otherwise random in translation and rotation, the interference function in terms of interatomic distances l is given by

$$\langle e^{i2\pi s \cdot l}\rangle = \frac{1}{2\pi}\int_0^{2\pi} e^{i2\pi sl\cos\alpha}\, d\alpha = J_0(2\pi sl).$$

FIG. 6. Linewidth versus s_0^2 for the (hk) reflections of a carbon fiber.
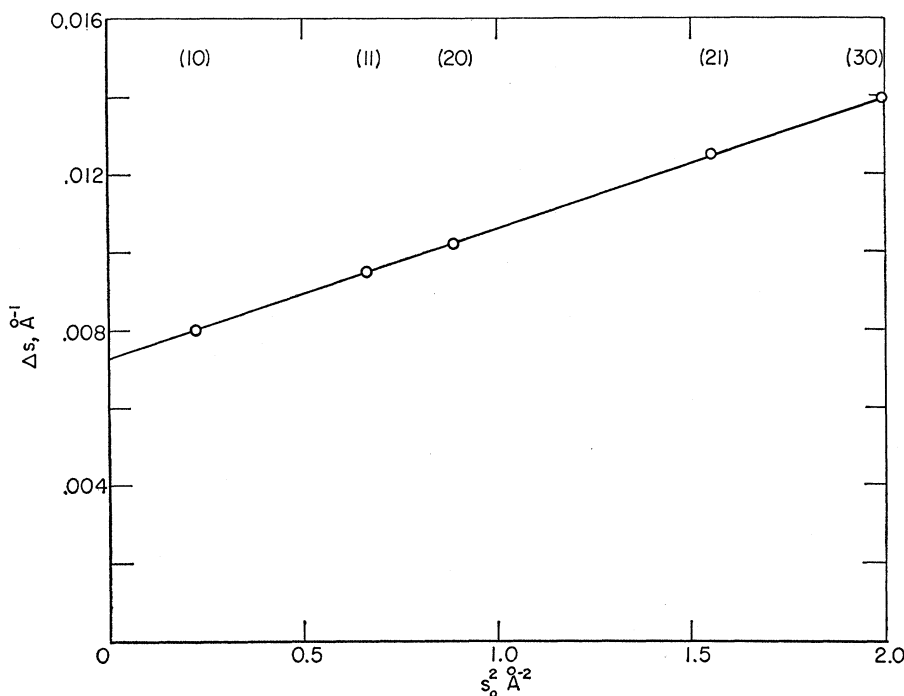
Equation (3) then takes the form

$$j(s) = 1 + \sum_q g(l_q)n(l_q)J_0(2\pi s l_q), \qquad (19)$$

where J_0 is the Bessel function of zero order. If $g(l)$ is replaced by $\epsilon_d(l)$, Eq. (19) would give intensities diffracted by disk-shaped layers under the conditions specified. Equation (19) is ideally suited for small or very defective layers. The coefficients of the Bessel terms can be obtained by a Bessel-Fourier transform of the intensities. As stated earlier, for sharp reflections we resort to lattice-sum technique and use Eq. (6) and those that follow it. In this situation, $j_0(s)$ is given by

$$j_0(s) = \sigma m F^2/16\pi s s_0, \qquad (20)$$

where σ is the atomic density (atoms/Å^2) of the layer, m is the multiplicity factor, and F^2 is the geometric structure factor.

An analysis of the profiles of the (100), (110), (200), (210), and (300) reflections of a carbon fiber showed them to be of Cauchy type and readily matched by Eq. (12) or (14). As outlined earlier, a plot of Δs versus s_0^2 gives a good indication whether the coefficients A_q are exponential. In Fig. 6 is shown a plot of Δs versus s_0^2 for all of the $(hk0)$ reflections studied. The fact that the points belonging to (100), (200), and (300) reflections fall on a straight line indicates a Gaussian distribution of distortion coefficient and an exponential form for A_q. The fact that the points belonging to (110) and (210) reflections fall on the same line indicates an isotropic distortion in the layers.

In Fig. 7 are shown $\ln\epsilon_q$ versus $L = q\bar{z}$ for cold-worked tungsten filings and for aluminum filed under liquid nitrogen (and measured at $-160°C$). The data are the intercept values of Warren's plots of $\ln A_q$ versus s_0^2 for different L's.[5] It is seen that $\ln\epsilon_q$ is linear with q; hence, A_q has an exponential form which is in accordance with Warren's observations that particle-size broadening is of a Cauchy type. The slope of the straight lines drawn correspond to the reciprocal of mean defect-free dis-
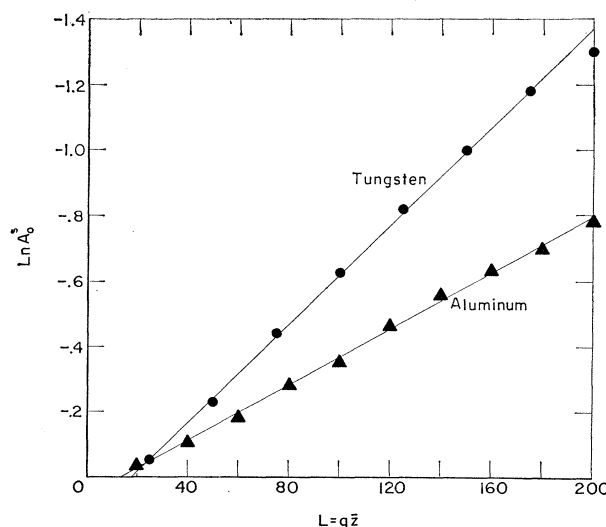

FIG. 7. $\ln A_0^s$ versus L for cold-worked tungsten and aluminum filings (data correspond to the intercept values of Warren's plots of A_L versus h_0^2) (Ref. 5).

tances, i.e., ~ 130 and ~ 230 Å for the tungsten and aluminum, respectively.

Warren observed that the materials studied were obviously not fragmented into small separate particles of sizes indicated by particle-size broadening equations. Instead, he contended, cold work has produced some sort of domain sturcture within the filing such that the different domains diffract essentially incoherently with respect to one another. The domain concept does not pretend to explain the form of A_q; however, it is physically unrealistic if A_q decreases exponentially with q, for as shown earlier, it implies that the largest number of domains are those containing single cells. It appears that if physical evidence is lacking for fragmentation or for the presence of domains having a reasonable size distribution, the concept of large defective domains is physically more realistic. The dimension that one should seek is not the particle size but the mean defect-free distance.

APPENDIX

We present a representation of interatomic distances l and the number $n(l)$ of neighboring atoms at a distance l from an atom.

1. Graphite-Like Layer Having a Bond Distance l_0

$l: l = l_0(p^2+q^2+pq)^{1/2}$, where p and q are integers such that $p>0$ and $p \geq q \geq 0$.

$$n(l): n(l) = \ 3, \quad \text{if } q=0 \text{ and } p \bmod 3 \neq 0$$
$$= \ 6, \quad \text{if } q=0 \text{ and } p \bmod 3 = 0$$
$$= \ 6, \quad \text{if } q=p$$
$$= \ 6, \quad \text{if } p \neq q \neq 0 \text{ and } (p-q) \bmod 3 \neq 0$$
$$= 12, \quad \text{if } p \neq q \neq 0 \text{ and } (p-q) \bmod 3 = 0.$$

We define $p \bmod q$ as the remainder when p is divided by q. In dealing with disk-shaped layers having a finite size, an upper limit $p_{\max}$ must be imposed on p. The upper limit modifies the conditions imposed upon p and

q in the set l as follows:

$$p_{\max} \geq p > 0,$$
$$\min\{p, \ (p_{\max}^2 - \tfrac{3}{4}p^2)^{1/2} - \tfrac{1}{2}p\} \geq q \geq 0.$$

For the finite size, $n(l)$ as defined above must be multiplied by $\epsilon(l)$ as defined by Eq. (5).

2. Diamond-Type Lattice Having a Bond Distance l_0

$l: l = l_0((p^2+q^2+r^2)/3)^{1/2}$, where p, q, r are all odd or all even integers with $p>0$. If odd, the additional conditions are $p \geq q \geq r$, if even, $[p \geq q \geq p \bmod 4$ and $q \geq r \geq (p+q) \bmod 4$ and $(r-(p+q) \bmod 4) \bmod 4 = 0]$.

If p, q, r are all odd,

$$\{n(l)\}, \text{ where } n(l) = 12, \quad \text{if } r=q \neq p$$
$$= 12, \quad \text{if } p=q \neq r$$
$$= 24, \quad \text{otherwise}.$$

If p, q, r are all even,

$$\{n(l)\}, \text{ where } n(l) = \ 6, \quad \text{if } r=q=0$$
$$= \ 8, \quad \text{if } p=q=r$$
$$= 12, \quad \text{if } p=q \text{ and } r=0$$
$$= 24, \quad \text{if } p=q \neq r \neq 0$$
$$= 24, \quad \text{if } p \neq q = r \neq 0$$
$$= 24, \quad \text{if } p \neq q \neq 0 = r$$
$$= 48, \quad \text{if } 0 \neq q \neq p \neq r \neq 0 \text{ and } r \neq q.$$

In dealing with spherical crystallites of finite size an upper limit $p_{\max}$ must be imposed on p. The conditions imposed upon p, q, r in the set l are as follows: If p, q, r are all odd, $q < p+1$, $p^2+q^2 < p_{\max}^2$, $r < q+1$, and $p^2+q^2+r^2 < p_{\max}^2$.

If they are even, $p \bmod 4 \leq q < p+1$, $p^2+q^2 < p_{\max}^2$, $(p+q) \bmod 4 \leq r < q+1$, $[r-(p+q) \bmod 4] \bmod 4 = 0$, and $p^2+q^2+r^2 < p_{\max}^2$. For the finite size, $n(l)$ defined above must be multiplied with $\epsilon(l)$ defined by Eq. (4).